Available online at www.sciencedirect.com
ScienceDirect
Journal of the European Ceramic Society 28 (2008) 2239–2246
www.elsevier.com/locate/jeurceramsoc

Visualisation of environmental degradation in ceramic superconductors using digital speckle photography

S. Recuero [a], M.T. Bona [b], N. Andrés [a], J.M. Andrés [b], L.A. Angurel [c,*]

[a] *Instituto de Investigación en Ingeniería de Aragón, Universidad de Zaragoza, c/Pedro Cerbuna 9, 50009 Zaragoza, Spain*
[b] *Instituto de Carboquímica, CSIC, c/Miguel Luesma 4, 50018 Zaragoza, Spain*
[c] *Instituto de Ciencia de Materiales de Aragón (CSIC-Universidad de Zaragoza), c/María de Luna 3, 50018 Zaragoza, Spain*

Received 16 November 2007; received in revised form 15 February 2008; accepted 29 February 2008
Available online 28 April 2008

Abstract

Differences in the environmental stability of Bi-2212 textured materials before and after annealing have been evaluated using digital speckle photography. This technique is able to provide information about the 2D evolution of the degradation processes by means of correlation coefficient reductions. The results indicate a faster degradation for as-grown samples. DSP detects this difference in very short times and allows determining the evolution of the process at any instant. The optical results were confirmed by analysing the differences in the samples microstructure and phase compositions by SEM-EDX, XRD and DRIFT techniques. All these techniques show that, in this material, environmental degradation process is associated with the chemical decomposition of the (Sr,Ca)CuO_2 phase.

PACS: 42.30.Ms; 74.72.Hs

Keywords: Speckle photography; Bi-2212; Superconductors; Degradation

1. Introduction

Superconducting materials could be an adequate selection in several technological applications. In the case of the ceramic high temperature superconductors, one of the main problems to analyse is their long-term stability because this is a factor that can limit their technological future. It is well known that $YBa_2Cu_3O_{7-\delta}$ (YBCO) compounds are more sensible to deterioration in diverse environmental conditions than $Bi_2Sr_2CaCu_2O_{8+\delta}$ (Bi-2212) ones.[1] In the Bi-2212 materials the general degradation mechanism is[2,3]:

$$Bi_2Sr_2CaCu_2O_8 + 3H_2O \rightarrow 2Sr(OH)_2 + Ca(OH)_2 + CuO + CuBi_2O_4$$

$$Sr(OH)_2 + CO_2 \rightarrow SrCO_3 + H_2O$$

$$Ca(OH)_2 + CO_2 \rightarrow CaCO_3 + H_2O$$

Initially, calcium carbonate becomes the predominant compound formed during degradation process. In a second stage, the strontium carbonate forms faster in a larger amount.[3]

High critical current densities have been obtained in textured Bi-2212 bulk materials using melting techniques; in particular, local melting induced with laser.[4,5] Due to the potential technological interest of these materials, it is important to characterize their humidity resistance. Like in other partial-melting processes used to fabricate Bi-2212 based tapes,[6] this laser process produces an incongruent melt and during solidification several phases appear.[7] In particular, $Bi_2Sr_2CuO_{6+\delta}$ (Bi-2201) and (Sr,Ca)CuO_2 are the main phases in the as-grown sample. After an adequate annealing, the Bi-2212 phase is recovered.[7,8] As a consequence of the phase segregation induced by the melting texturing technique the annealed samples shows a layer close to the surface where the amount of (Sr,Ca)CuO_2 is important.[7]

The stability in water environment of multi-phase Bi-2212 materials was previously studied.[9] After having exposed the samples to an aerated and deionised water solution for several days, it was observed that degradation problem was not associated with the Bi-2212 phase, which remained stable after 7 days in a water solution. Degradations reactions start in the

* Corresponding author.
E-mail address: angurel@unizar.es (L.A. Angurel).

0955-2219/$ – see front matter © 2008 Elsevier Ltd. All rights reserved.
doi:10.1016/j.jeurceramsoc.2008.02.024

$(Sr,Ca)CuO_2$ phase that reacts with water molecules and completely decompose in $CuSr_2(OH)_4$, CuO, $SrCO_3$ and $Ca(OH)_2$.

In this work, the environmental stability of as-grown and annealed textured Bi-2212 samples in high humidity atmospheres have been studied using digital speckle photography. This technique has been used to study random processes at rough surfaces in different materials.[4,10] Conclusions about differences in local degradation rates can be obtained in very short times.

2. Experimental

2.1. Sample preparation

Precursor monoliths have been prepared by isostatic pressure of commercial Bi-2212 powders provided by Nexans Superconductors. The surface of the precursors was textured using a high power diode laser adapted to obtain textured samples in planar geometries.[4,5] The total laser power used during the melting process was 12 W and the texturing speed was 25 mm/h. Samples have been annealed in air at 845 °C for 60 h and at 800 °C for 12 h. After this thermal treatment, samples were cooled inside the furnace until 600 °C and then quenched.

2.2. Microstructure characterization

As-grown and annealed superconductor samples of 0.8 cm × 1 cm were prepared for their microstructure characterization. It involved diffuse reflectance infrared spectroscopy (DRIFT), X-ray diffractometry (XRD) and scanning electron microscopy (SEM). The samples were analysed prior the treatment and subsequently introduced in a climate chamber for different time intervals at a controlled atmosphere of 25 °C and 90% relative humidity. The periods of moisture treatment studied were 1, 5, 15, 30 min, 2.5 h, 10.5, 26.5 and 90.5 h. A dried-chamber with silica gel at the bottom was used to protect the material from ulterior environmental degradation. The samples were analysed after each time interval.

2.2.1. DRIFT

DRIFT spectra were recorded on a Bruker-Tensor 27 FTIR spectrometer equipped with a Globar source, potassium bromide beamsplitter and a La-DTGS detector. Two purge connectors provided separately the interferometer and sample compartment with CO_2-free dry air.

A diffuse reflectance sample cup (13 mm diameter) was used for the acquisition of the spectra. Once placed the sample into the compartment, the space around the sample was filled with potassium bromide. Then, it was placed into the diffuse reflectance accessory to acquire the spectrum using the same halide (KBr) as reference material. Spectra obtained were the result of co-adding 64 scans over the range 400–4000 cm^{-1} performed at 1 cm^{-1} of digital resolution. All the spectra were acquired in absorbance mode, viz. log(1/reflectance).

2.2.2. XRD

Phase composition close to the surface of the sample was determined by X-ray diffraction analysis using a Bruker D8-Advance devise with a θ–θ configuration, Cu Kα radiation, graphite as a secondary monochromator and a scintillation detector. The XRD patterns were made from the surface of bulk sample, at room temperature and the range covered from $2\theta = 3$–50 with a Bragg angle step of 0.05° and 1 s time/step. The identification analysis of the different crystalline species

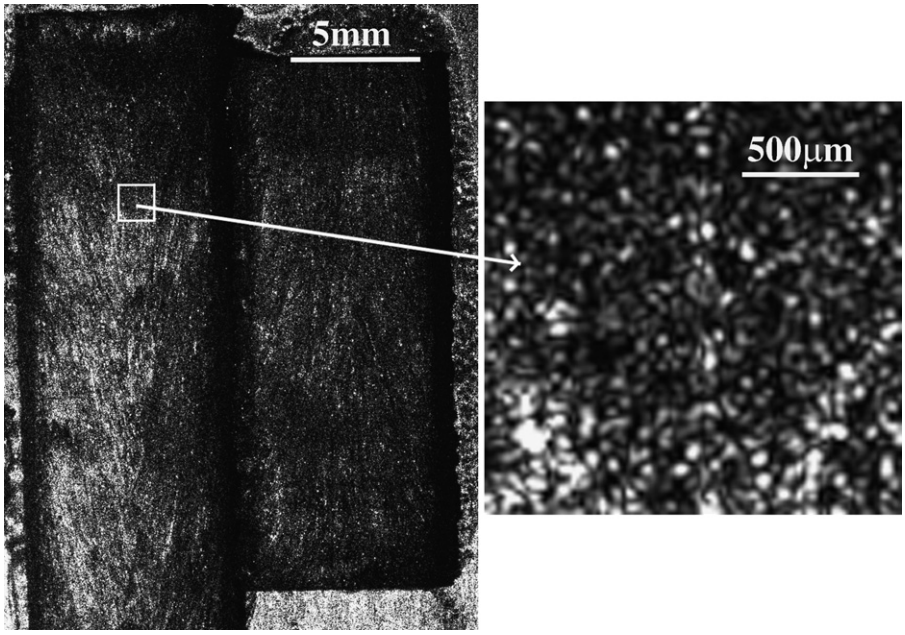

Fig. 1. Photograph of the samples illuminated with a coherent light: as-grown (left) and annealed (right) samples. In the inset, a part of the photograph with a higher resolution is presented in order to show the speckle.

found in the studied samples was performed using DIFFRACplus EVAv8.0 software.

2.2.3. SEM

The surface microstructure has been studied by means of scanning electron microscopy in a Hitachi S-3400 N microscope equipped with a Si/Li detector for energy dispersive X-ray (EDX) analysis Röntec XFlash. Both phase composition (backscattered electrons) and morphology (secondary electrons) were used for the study.

2.3. Digital speckle photography

The samples are fixed to an aluminium plate with GE varnish. After having confirmed that the samples do not move, the system is placed inside a small chamber with a relative humidity value of a 93%. They are illuminated with a collimated laser beam under an angle $\theta = 15^\circ$ and imaged onto a CCD camera. The reflected light from the rough surface under coherent illumination generates speckle fields (Fig. 1) that contain all the information about the surface microstructure. The images are taken at different times while changes in the surface take place. Each image can be compared with the image in the reference state.

In the case of surface analysis, a quantitative measure of the similarity of the speckle patterns in two situations is introduced by the definition of the correlation coefficient:

$$c_{1i} = \frac{\langle I_1 I_i \rangle - \langle I_1 \rangle \langle I_i \rangle}{\left[(\langle I_1^2 \rangle - \langle I_1 \rangle^2)(\langle I_i^2 \rangle - \langle I_i \rangle^2) \right]^{1/2}} \quad (1)$$

where I_1 and I_i are the intensities at each recorded image at the reference and at the instant i, respectively, and the angle brackets denote the spatial average in the image. A 2D detailed information about surface modifications can be obtained by calculating the correlation coefficient in several sub-regions of the image. In this work, square regions of 16×16 pixels have been considered.

3. Surface modifications associated with environmental degradation

In order to facilitate the comparison between as-grown and annealed samples, two samples have been glued together as it is shown in Fig. 1. Sample photographs were taken every 10 s using an exposition time of 15 ms and an aperture of 16. The inset of Fig. 1 shows the speckle of the photograph that contains all the information of the surface microstructure.

The evolution of the surface can be monitored through the changes in the 2D correlation maps. Fig. 2 shows some examples of these 2D correlation maps at different times. It is clearly observed that the correlation is lost faster in the as-grown sample indicating a faster surface degradation. In order to quantify this

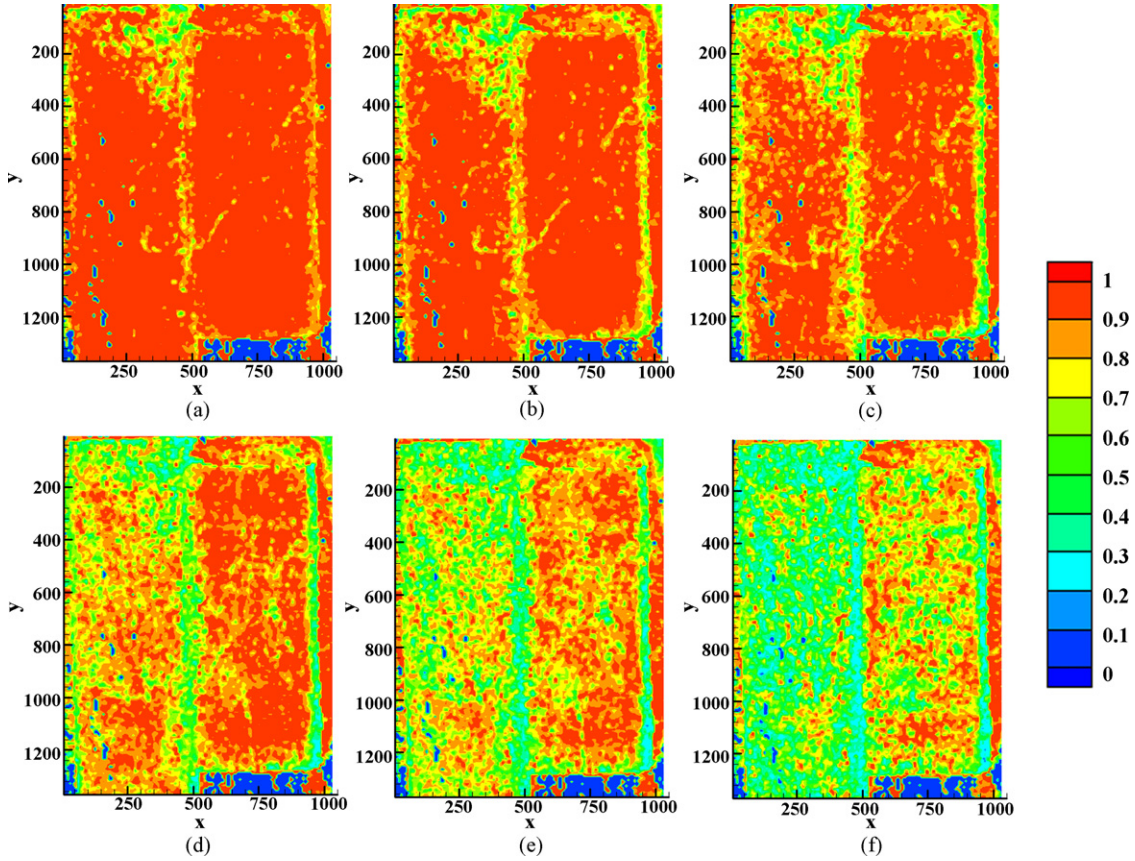

Fig. 2. 2D correlation maps of the as-grown and annealed samples after different times in a high humidity atmosphere: (a) $t = 30$ s, (b) $t = 60$ s, (c) $t = 100$ s, (d) $t = 160$ s, (e) $t = 260$ s and (f) $t = 660$ s.

difference the correlation coefficient of the image has been quantified and the results during 1 h in high humidity atmosphere are presented in Fig. 3. The correlation coefficient of the as-grown sample reduces until a value of 0.37. In the annealed sample this reduction finishes at a value of 0.66. If the reduction rate of the correlation coefficient is calculated in the region between 1 and 0.75 it is possible to conclude that the as-grown sample deteriorates near four times faster than the annealed one.

These differences between as-grown and annealed samples are confirmed by SEM, XRD and DRIFT analytical techniques. Attending to scanning electron microscopy, the surface morphology evolution of the two samples along moisture treatment is shown in Fig. 4. As it can be observed, the advancing surface modification is faster in the as-grown sample than in the annealed one, leading to a final swollen striated material spread all over the sample. Besides the speed of the surface modification, a higher extension is affected in as-grown samples.

One of the main differences between as-grown and annealed samples is that in the first one the amount of $(Sr,Ca)CuO_2$ phase

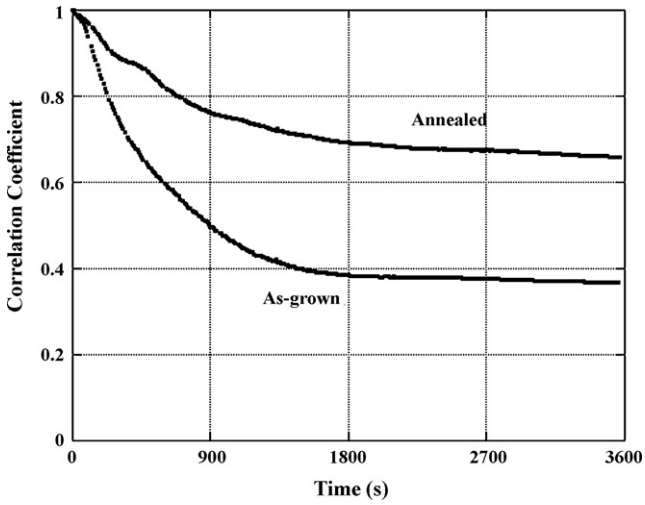

Fig. 3. Evolution of the correlation coefficient with time in the two samples.

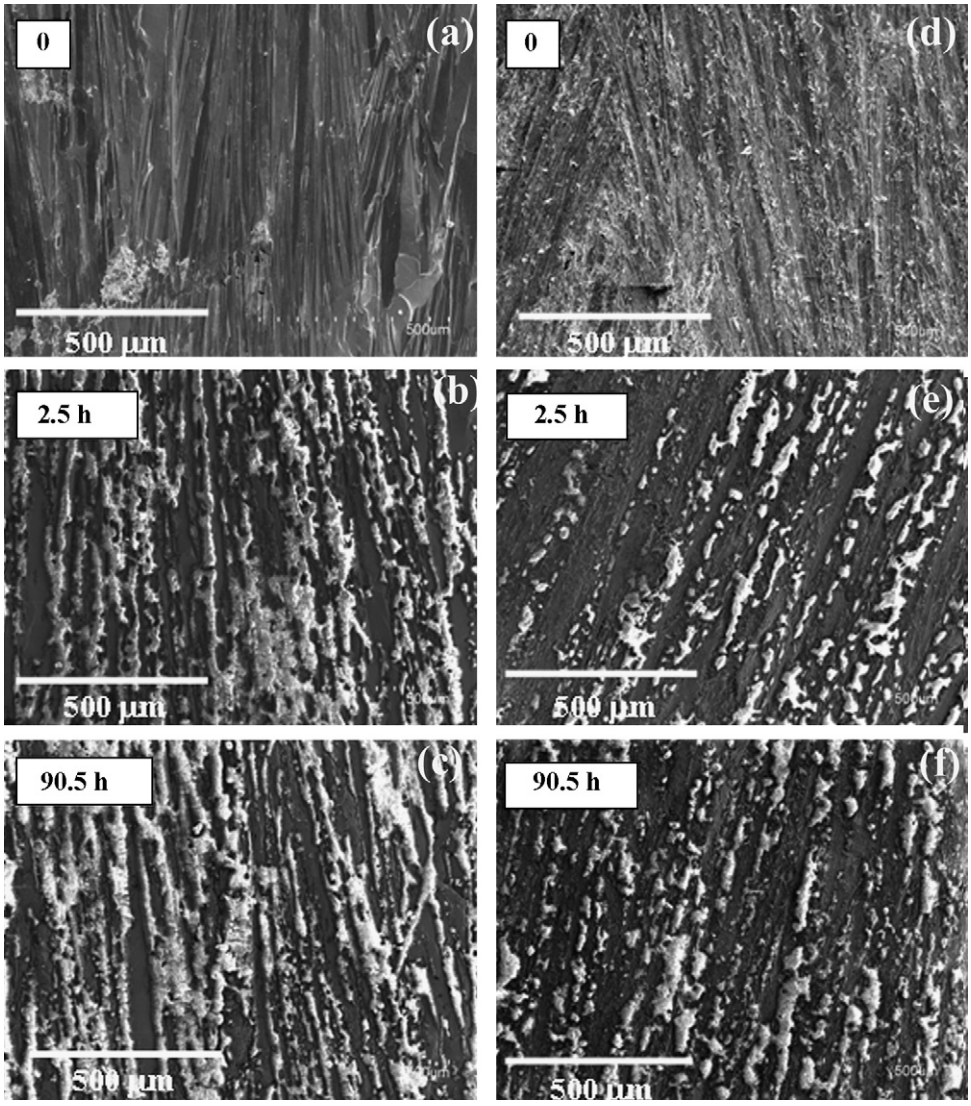

Fig. 4. Morphology of the surface of the as-grown (a–c) and annealed (d–f) samples after different times in the high humidity atmosphere.

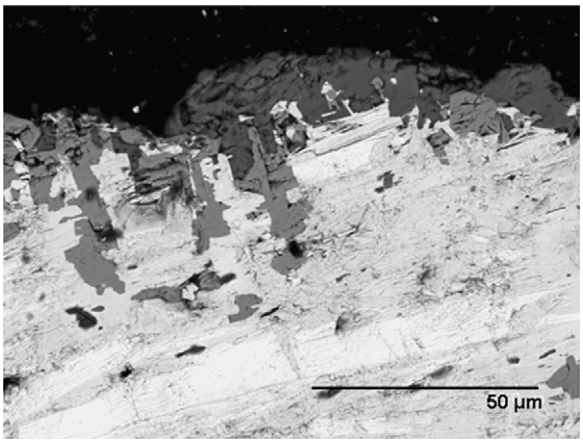

Fig. 5. SEM micrograph of the transversal section of the as-grown sample after 90.5 h in the high humidity atmosphere. The decomposition of the (Sr,Ca)CuO_2 phase is observed.

is higher[5] and it is expected that this is the phase responsible of the environmental degradation.[9] This has been confirmed studying the cross-section of both materials. As an example, Fig. 5 shows this cross-section in the as-grown sample. The (Sr,Ca)CuO_2 grains that are close to the surface start to decompose to an amorphous phase that is responsible of the swollen regions that are observed in Fig. 4. The analysis of this phase shows that its cationic stoichiometry is very similar to the original one. The reactivity of this phase is corroborated by XRD analysis where peak intensities associated to mixed oxides reduce drastically during the first 30 min moisture treatment both in as-grown and annealed samples, without the appearance of new crystalline species (Fig. 6). The complete depletion of the (Sr,Ca)CuO_2 phase does not occur even though moisture treatment took 90.5 h. On the other hand, Bi-2201 and Bi-2212 phases remain inalterable all along the treatment. In order to understand the XRD patterns it is important to have in mind that scale of the peaks in both samples is different. The base line is similar in both samples and it has not changed during the experiments.

The characterization of the chemical reactions that take place during the decomposition in humid atmosphere is completed by the evolution of the DRIFT spectra (Fig. 7). This analytical technique is able to detect the appearance of new species into the surface of the material. These changes, as it is observed in other techniques, occur faster for as-grown than annealed samples. The existence of new compounds could confirm their amorphous nature and consequently their lack in XRD patterns. Moreover, these results are in agreement with the fact that the process is faster at the initial stages to reduce gradually at longer times. As it is showed in SEM photographs, the surface is partially covered with a new material that would make difficult the diffusion of H_2O and CO_2 into the bulk.

When the new absorption bands are studied along the process, it can be observed the presence of hydroxyl functional groups during the initial stage of (Sr,Ca)CuO_2 degradation. They can be due to the formation of $M(OH)_2$ (M = Ca, Sr). Although previous studies describe the synthesis of each compound, in

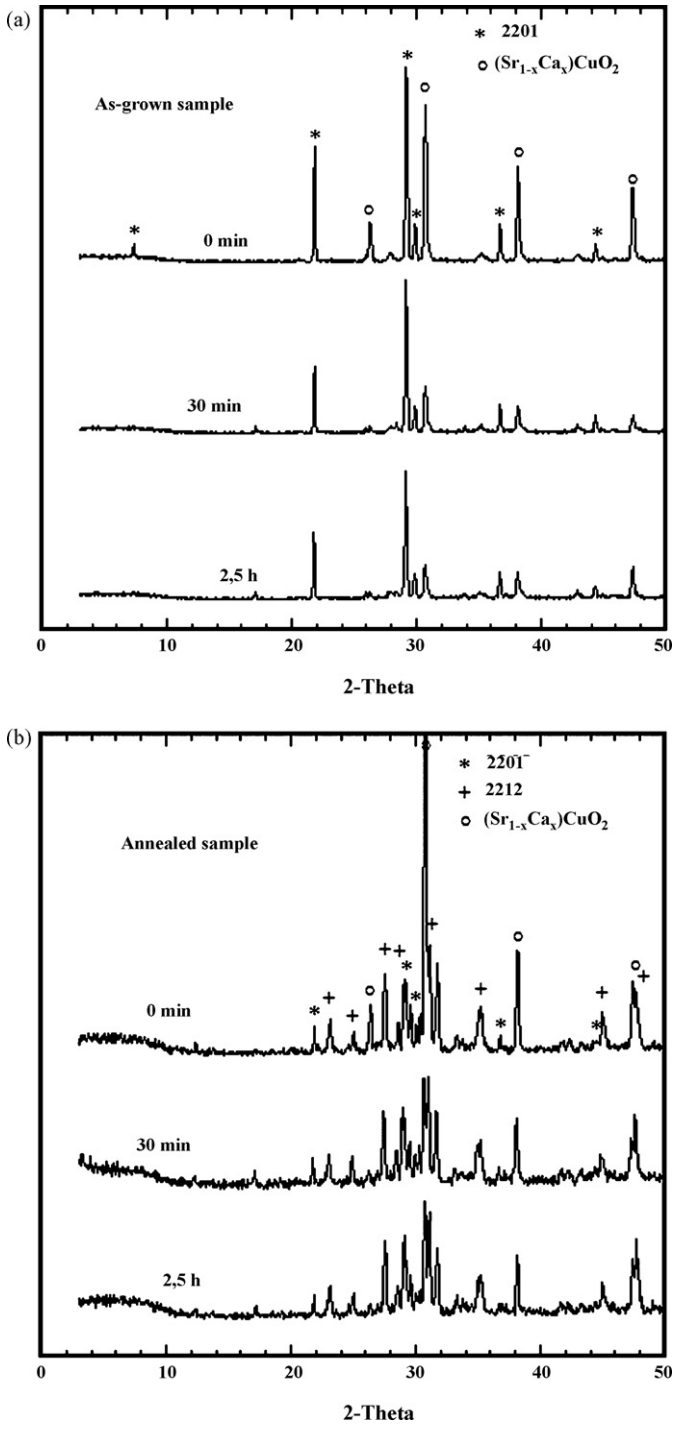

Fig. 6. Evolution of X-ray spectra of the as-grown (a) and annealed (b) samples.

this case the great overlaps and the very low signal-to-noise (S/N) ratio present in the spectra difficult the band assignations. Even so, it is possible to distinguish between stretching vibrational modes of free and hydrogen-bonded OH ion groups at 3610 and 3510 cm^{-1}, respectively, present in $M(OH)_2$ compounds, and an absorption band at 3400 cm^{-1} assigned to the hydrogen-bonded OH ion groups of $M(OH)_2 \cdot H_2O$. This band finally overlaps with the one associated to OH stretching vibrations of adsorbed or crystallized water molecules at 3300 cm^{-1}.

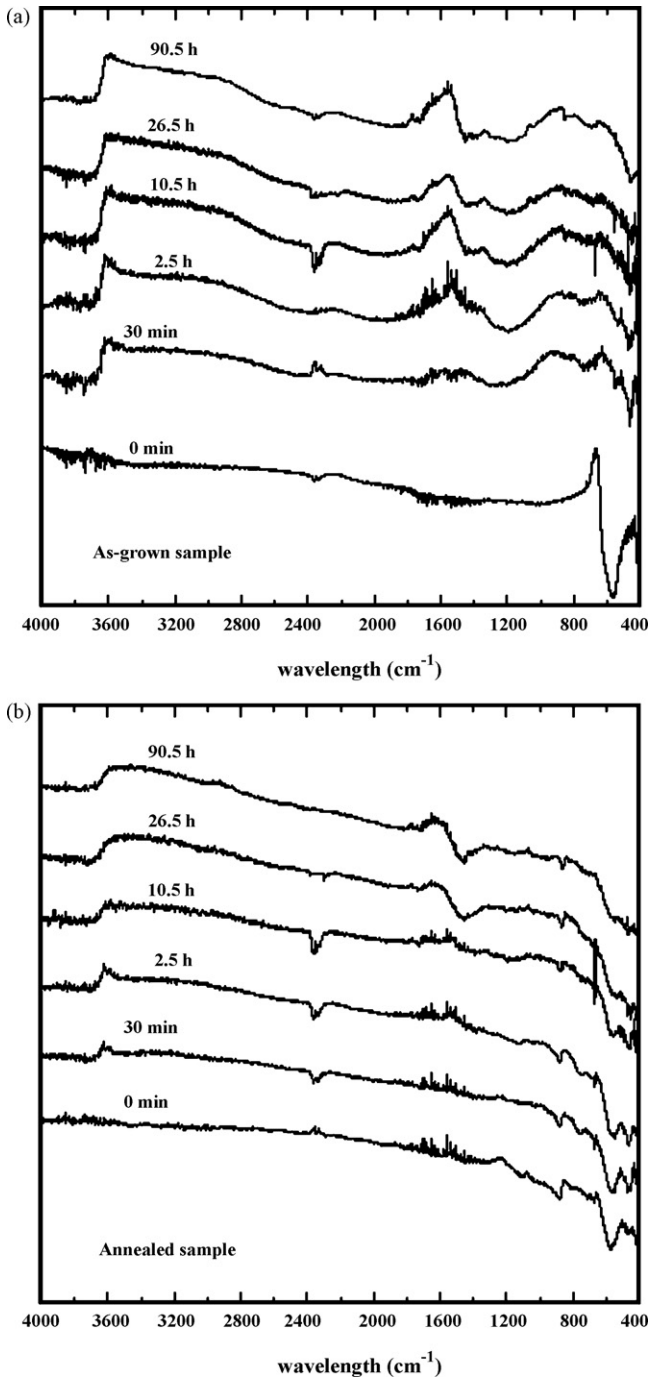

Fig. 7. Evolution of DRIFT spectra of the as-grown (a) and annealed (b) samples.

Whereas the as-grown sample shows the maximum overlap after a treatment of 26.5, 90.5 h are required for the annealed one as it can be observed in Fig. 7. Simultaneously to hydroxyl compounds synthesis, some variations are observed in the region around 620 cm^{-1} assigned to in-plane stretching Cu–O bond in CuO_2 layers. Its intensity upon aging reduces at the same time as new bands at 1300–1700 cm^{-1} region appears assigned to CuO compound. The logical evolution of $M(OH)_2$ compounds in presence of H_2O and CO_2 is the synthesis of carbonate species. Thus, as moisture treatment progresses, absorption bands related to those compounds appear at 1600 and 1750 cm^{-1}. Despite its low intensity, the isolation of the last one assigned to carbonate combination modes, facilitates the characterization of this compound. It is also observed how absorption band intensity associated to hydrogen-bonded OH ion group present in $M(OH)_2$ at 3510 cm^{-1} decrease in as-grown sample as carbonate compounds are formed.

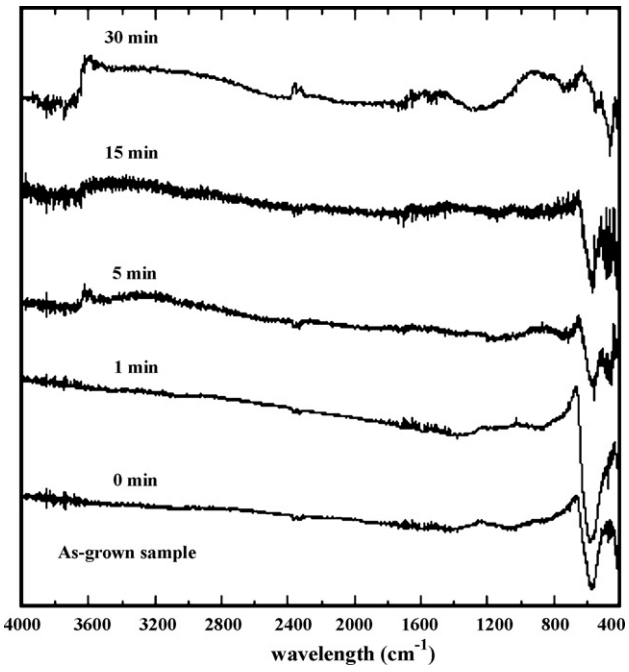

Fig. 8. Evolution of DRIFT spectra of the as-grown sample during the initial stages of the environmental degradation.

All these experiments are complementary. The advantage of DSP is that it allows obtaining conclusions about degradation evolution faster than the other techniques. Most of the differences between both samples can be inferred in the initial 30 min. For this reason, a new set of samples was prepared to study morphological changes during that period of time. Samples with exposition to a high humidity atmosphere for 1, 5 and 15 min have been analysed. Although DSP analysis shows that degradation has started in the annealed sample the other techniques have not detected any modification. In the case of the as-grown sample the DRIFT spectra detects the initial stage for water adsorption and the subsequent synthesis of $M(OH)_2$ in the sample with a 5 min treatment (Fig. 8). Surface changes have been also detected in SEM micrographs.

4. Additional information obtained from DSP experiments

One of the main advantages of digital speckle photography is that it is possible to obtain information of the local behaviour of the degradation process. This information can be obtained with more detail if a higher magnification is used. As the degradation process is associated with the decomposition of the $(Sr,Ca)CuO_2$ phase, the mapping of the degradation should reflect the surface grain alignment. This is reflected in Fig. 9 where the 2D correlation coefficient map in the as-grown sam-

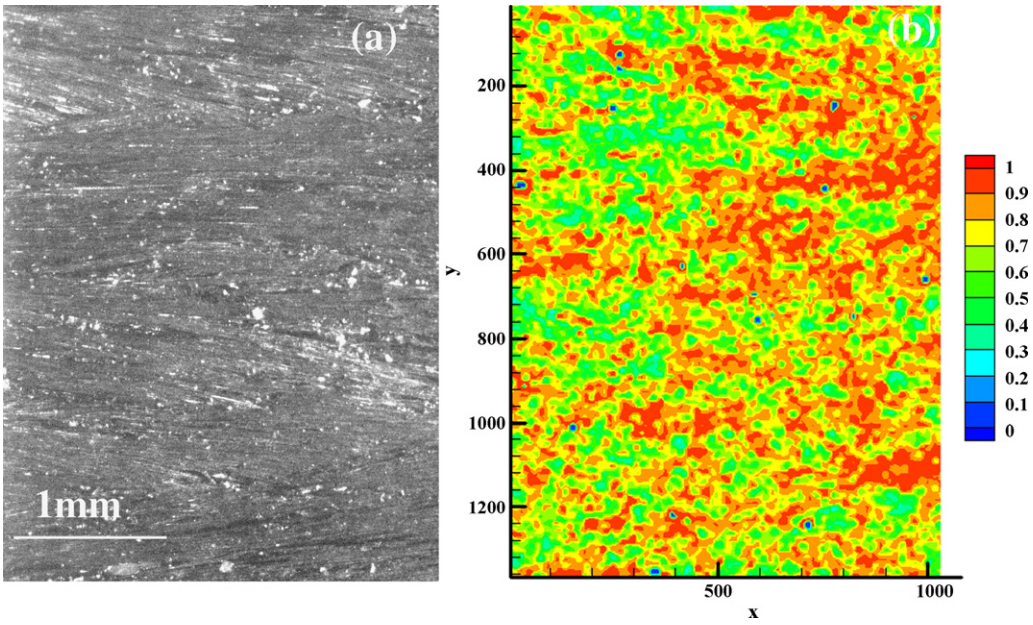

Fig. 9. (a) Speckle photograph of the as-grown sample with a higher magnification. (b) 2D map of the correlation coefficient after 30 s.

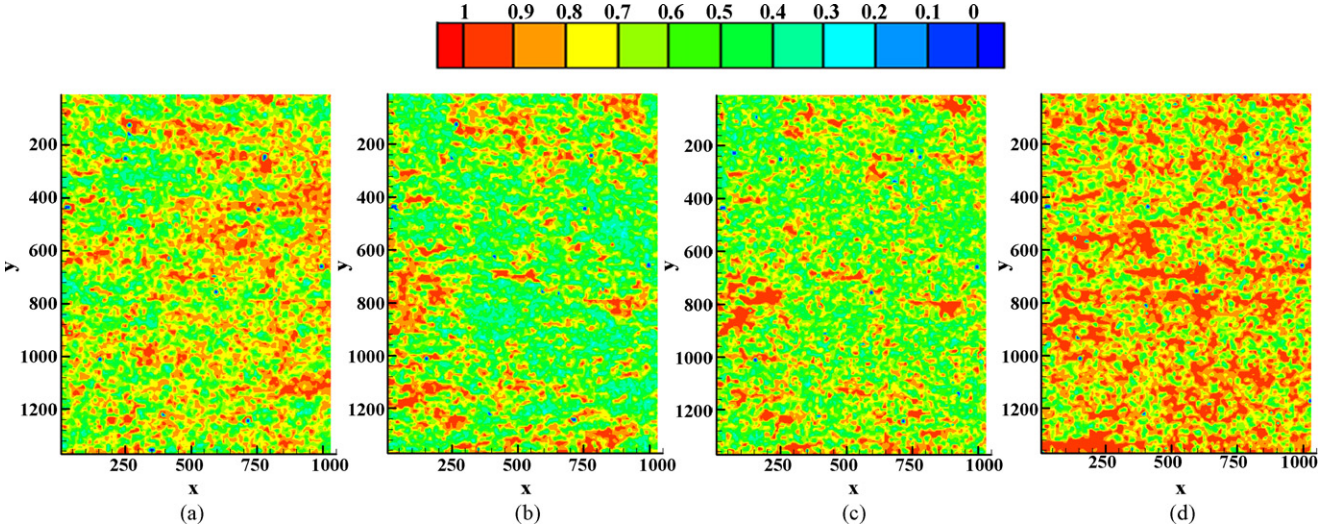

Fig. 10. 2D correlation coefficient maps of the as-grown sample after 40 s taking as reference: (a) the image at 1 s, (b) the image at 200 s, (c) the image at 800 s and (d) the image at 1500 s.

ple after 30 s in a high humidity atmosphere is presented with the speckle photograph. In this magnification conditions each pixel corresponds to 2.7 μm in the sample. The 2D map clearly shows the same trends presented by the sample microstructure.

Another important fact is that DSP allows to analysing how the degradation process evolves at any instant by changing the reference. Taking the reference at an instant t the correlation maps will show how the surface has modified from this instant. Fig. 10 shows the 2D maps of the as-grown sample after 40 s taking the reference at different instants: 1, 200, 800 and 1500 s. The first conclusion that can be derived from these images is that the surface degradation rate is higher at 200 s becoming smaller at higher times. A second conclusion is that in the initial image the degradation process follows the surface microstructure, while in the other images the process is more uniform. These images also show where the degradation process is taking place at any instant. For instance, in the bottom left corner it is possible to observe that the degradation is faster after 200 s (region in the image that corresponds to the lower correlation coefficient values) and that this process has completely stopped after 1500 s, because in this image, this region maintains a correlation coefficient value close to 1.

5. Conclusions

Digital speckle photography is an adequate technique to characterize environmental degradation in high temperature superconducting materials. In the case of as-grown and annealed

textured Bi-2212 monoliths, DSP shows that degradation rate is nearly four times faster in the as-grown sample. This difference can be deduced in very short times.

XRD, SEM and DRIFT have been used for analysing the nature of the chemical reactions that are responsible of the surface modifications. These techniques have confirmed that degradation with water is associated to chemical decomposition of the (Sr,Ca)CuO_2 phase, present in multi-phase Bi-2212 materials. A swollen striated surface appears all over the surface wherein mixed oxide phase degrades to $SrCO_3$, $CaCO_3$ and CuO.

Another advantage of DSP experiments is that it allows analysing how the degradation process evolves. This information can be derived locally, determining in which part of the sample the surface modifications are taking place at any instant.

Acknowledgements

This research was supported by the Spanish Ministerio de Educación y Ciencia (MAT 2005-06279-C03-01, -02 and -03) and by the Gobierno de Aragón (G.I.C., Laser Optical Technology and Applied Superconductivity groups). One of the authors M.T. Bona (CSIC-I3P) wishes to thank the FSE for financial support.

References

1. Argyropoulou, R., Ochsenkühn-Petropoulou, M., Dounis, C., Karaboulis, P., Altzumailis, A. and Ochsenkühn, K. M., *J. Mater. Process. Technol.*, 2007, **181**, 2–5.
2. Jin, S. G., Zhu, Z. Z., Liu, L. M. and Huang, Y. L., *Solid State Commun.*, 1990, **74**, 1087–1090.
3. Lee, D., Condrate Sr., R. A. and Taylor, J. A., *Phys. C*, 2001, **350**, 1–16.
4. Angurel, L. A., Diez, J. C., de la Fuente, G. F., Gimeno, F., Lera, F., López-Gascón, C., Martínez, E., Mora, M., Navarro, R., Sotelo, A., Andrés, N., Recuero, S. and Arroyo, M. P., *Phys. Status Solidi A-Appl. Mater. Sci.*, 2006, **203**, 2931–2937.
5. Mora, M., Gimeno, F., Angurel, L. A. and de la Fuente, G. F., *Supercond. Sci. Technol.*, 2004, **17**, 1133–1138.
6. Ray, R. D. and Hellstrom, E. E., *Phys. C*, 1991, **175**, 255–260.
7. Mora, M., Martínez, E., Díez, J. C., Angurel, L. A. and de la Fuente, G. F., *J. Mater. Res.*, 2000, **15**, 614–620.
8. Natividad, E., Díez, J. C., Angurel, L. A. and Andrés, J. M., *J. Am. Ceram. Soc.*, 2004, **87**, 1216–1221.
9. Zhou, J. P., McDevit, J. T. and Hazeltn, D., *Supercond. Sci. Technol.*, 1999, **12**, 601–605.
10. Hinsch, K. D., Frike Begemann, T., Gülker, G. and Wolff, K., *Opt. Lasers Eng.*, 2000, **33**, 87–105.